S. Machida, T. Miyata†, Y. Hagiwara‡, H. Yoshinari*, and Y. Suzuki**

A Statistical Study of the Effect of Local Brittle Zone (LBZ) on the Fracture Toughness (CTOD) of Weldments

REFERENCE Machida, S., Miyata, T., Hagiwara, Y., Yoshinari, H., and Suzuki, Y., **A statistical study of the effect of local brittle zone (LBZ) on the fracture toughness (CTOD) of weldments**, *Defect Assessment in Components – Fundamentals and Applications*, ESIS/EGF9 (Edited by J. G. Blauel and K.-H. Schwalbe) 1991, Mechanical Engineering Publications, London, pp. 633–658.

ABSTRACT The paper presents the experimental heat affected zone (HAZ) crack tip opening displacement (CTOD) data in terms of the size and number of local brittle zones (LBZs) hit by fatigue pre-crack which was carried out by the Fracture Toughness of Weldments (FTW) Committee of the Japan Welding Engineering Society (JWES). The data plots of the critical CTOD versus LBZ size lead to the observations that the so-called 'LBZs', which include coarse grain HAZ (CGHAZ), subcritically reheated coarse grained HAZ (SRCG), intercritically reheated CGHAZ (IRCG), and tempered IRCG (TIRCG), have fracture toughness values (δ_c) with large scatter, but the mean value $\bar{\delta}_c$ seems to be represented by a function of LBZ size. The relation between δ_c and LBZ size may differ from one type of LBZ to another, but due to rather small number of valid experimental data the above relationship was assumed same for all types of LBZ except TIRCG which was shown to resume its toughness considerably by tempering effect. A probabilistic model is proposed which consists of $\bar{\delta}_c$, the average value of δ_c versus LBZ size, the Weibull type distribution of δ_c for a given $\bar{\delta}_c$, the experimentally obtained probability of size of an individual LBZ and that of number of LBZs hit by a fatigue precrack of CTOD specimen, and assumes that the smallest δ_c out of probabilistically determined δ_c for individual LBZ hit by a fatigue precrack controls the overall δ_c of a HAZ CTOD specimen (weakest link concept). Numerical simulations based on this model compared well with the experimental results. API requirement on HAZ CTOD testing is discussed on the basis of numerical simulations. Plate thickness effect is predicted taking mechanical and metallurgical contributions into account.

Introduction

It was found in the early eighties that CTOD testing on the welded joint of the steels used for offshore structures occasionally showed very low level of fracture toughness in terms of critical CTOD. It had been well known that small local brittle zones (LBZs) actually existed in HAZ of the conventional C–Mn steels. But the above findings forced the fabricators and the users to have renewed concern about material selection and welding procedure.

Fortunately, no serious accidents of offshore structures directly caused by LBZ have occurred yet, but there still prevails an anticipation that some vicious combination of unfavourable conditions may lead to a catastrophic failure. The CTOD testing, which is considered to be more sensitive to LBZ than the Charpy 'V' testing, is now becoming one of the routine testings

* Department of Naval Architecture and Ocean Engineering, University of Tokyo, Japan.
† Department of Materials Science Engineering, Nagoya University, Japan.
‡ Research and Development Laboratory, Nippon Steel Corporation, Sagamihara, Kanagawa, Japan.

required by specifications and/or codes for the selection of materials and qualification of welding procedures **(1)–(3)**.

On the other hand, the significance of existence of LBZ has not been well clarified yet. Some engineers claim that HAZ CTOD testing required by codes and/or specifications (e.g., API–RP2Z) is unnecessary and meaningless because it leads to unrealistically stringent toughness requirement.

This paper is not intended to answer the above argument but to propose a probabilistic model of the critical CTOD, which depends on LBZ size and number of LBZ hit by a fatigue precrack. The experimental results of HAZ CTOD testings (3PB test) carried out by the FTW Committee of the Japan Welding Engineering Society were analysed using the model and compared well with the numerical simulations. The effect of LBZ on CTOD, i.e., which of the total size and an individual size of LBZs points to low CTOD, is discussed. Meaning of the requirement of API–RP2Z for HAZ CTOD testing is also discussed and a method to evaluate a conservative estimation of HAZ CTOD is suggested. The plate thickness effect considering both mechanical constraint and probability of existence of LBZs is also discussed.

Experiment

The base metal used for testing was 50 mm thick 500 N/mm^2 class high strength steel plate normally used for offshore structures and is equivalent to BS 4360–50E. Chemical composition and mechanical properties are shown in Table 1. The overmatched welded joints, 'X' and 'K', with SAW weld pass sequence are schematically shown in Fig. 1. Every pass was layed with almost

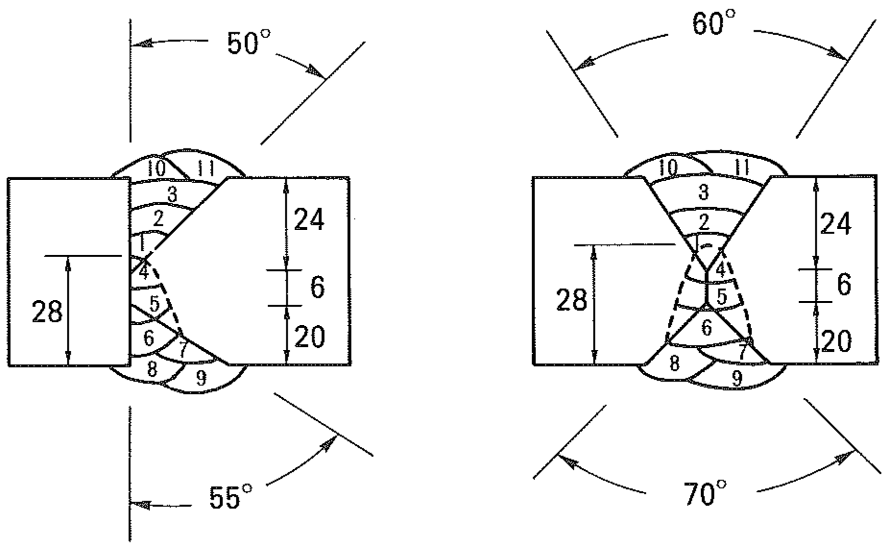

(a) K–weld joint (b) X–weld joint

Fig 1 Weld pass sequence of 'K' and 'X' weld joint

Table 1 Chemical composition and mechanical properties of steel used

Steel grade	*Thickness*	*Chemical composition (wt percent)*							*Mechanical properties*		
		C	*Si*	*Mn*	*P*	*S*	*V*	*Nb*	*Y.P. (N/mm^2)*	*T.S. (N/mm^2)*	*Elong. (%)*
BS 4360–50 E	50 mm	0.08	0.34	1.44	0.003	0.001	0.003	0.024	518	586	28

Table 2 Welding conditions of SAW

Welding method	*Current (Amps)*	*Voltage (V)*	*Speed (cm/min)*	*Heat input (kJ/cm)*
Submerged arc welding	850	31 ~ 33	26 ~ 30	56 ~ 64

same welding conditions as shown in Table 2. The B × 2B three-point bend specimens for CTOD testing were made. Through thickness machined notch with fatigue pre-cracking after local precompression (platen diameter $\gtrsim 2/3B$, compressive plastic strain = 0.8 ~ 1.2 percent) was made to hit the specified LBZ in each of the specimens. An example of macro-etched photograph is shown in Fig. 2 for a 'K' joint. The test temperature of −60°C was chosen based on the results of a series of tests to obtain the transition curve. The temperature of −60°C is about in the middle of transition temperature zone.

The scatter of CTOD data obtained from 13 to 20 specimens tested at −60°C for 'X' and 'K' welded joints, respectively, is shown in Fig. 3 in terms of the Weibull plot. At this temperature all the critical CTOD values were δ_c by way of BS 5762 5 notation. Both data approximately fit to the two parameter Weibull type distribution. The smaller scatter of 'X' joint (larger shape parameter of Weibull distribution) could be attributable to the smaller number

Fig 2 An example of macro-etched photograph

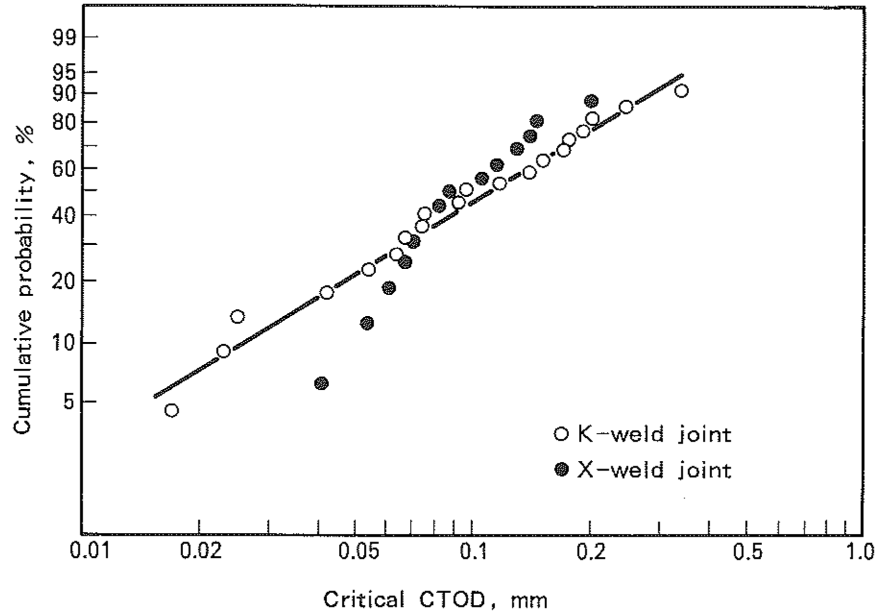

Fig 3 Scatter in CTOD values of 'K' and 'X' weld joint at −60°C (Weibull plot)

of LBZ hit by a fatigue precrack in 'X' joints as compared to 'K' joints which normally have a fairly straight weld fusion line.

Identification of microstructures in HAZ (4)

Figure 4 shows an example of the results of metallurgical microstructure identification which was made through heat flow analysis using the Adams' equation (5) given by

$$\frac{1}{\theta_{max} - \theta_0} = \frac{4.13c\rho}{(q/u)}\, y + \frac{1}{\theta_m - \theta_0} \tag{1}$$

where

θ_{max} = maximum temperature attained
θ_0 = initial temperature
q = heat-input per unit plate thickness
y = a distance from weld fusion line
θ_m = melting temperature
c = specific heat
u = welding speed
ρ = density

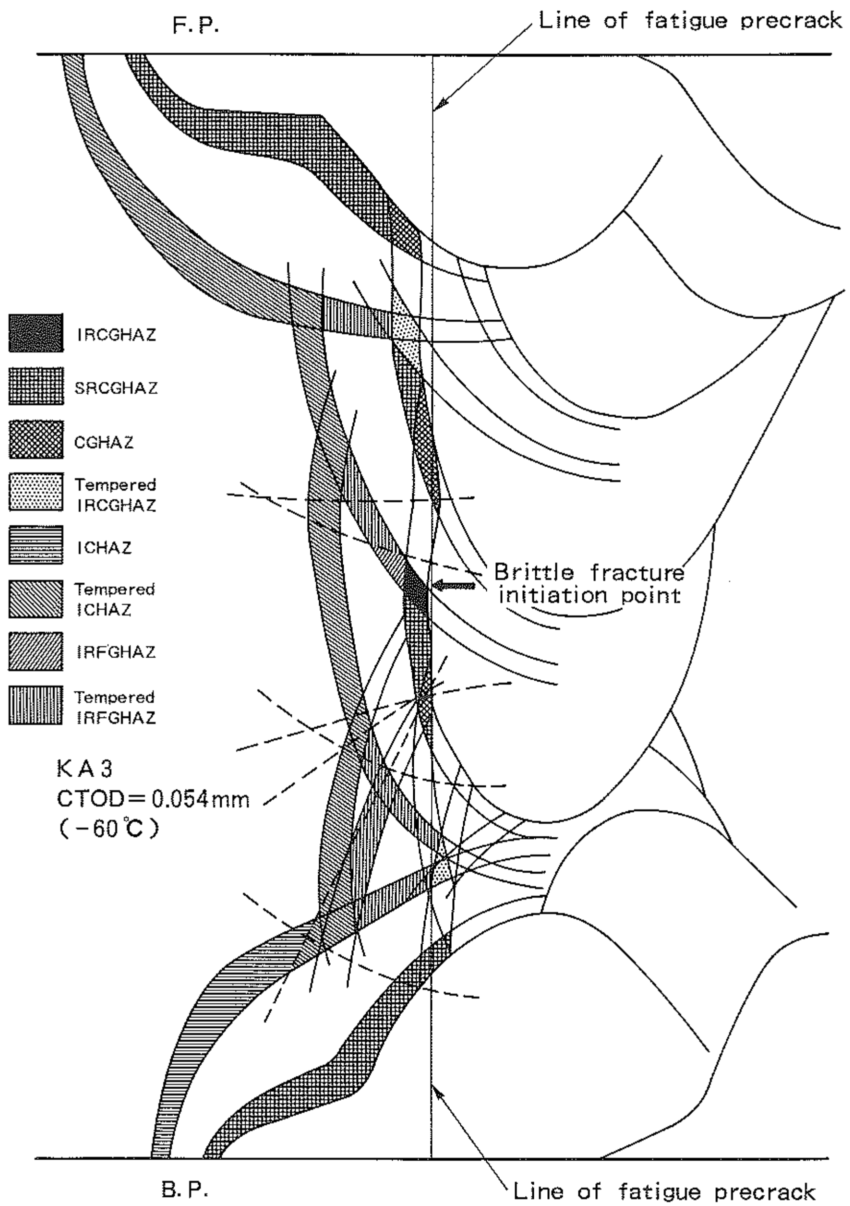

Fig 4 An example of metallurgical microstructure identification by heat flow analysis

Equation (1) was simplified to

$$\frac{1}{\theta_{max} - \theta_0} = A \cdot y + \frac{1}{\theta_m - \theta_0} \tag{1a}$$

where A is a constant. The value of A is determined by setting $\theta_{max} = 900°C$, $\theta_m = 1550°C$, $T_0 = 200°C$ and y = HAZ width.

From the above heat flow analysis, eight regions subjected to different heat cycles were identified as shown in Fig. 4. The microstructures produced by the first and a subsequent pass (double heat cycles) are classified into four kinds of coarse grain zone as shown schematically in Fig. 5 **(6)**. Eventually the following four microstructures were adopted as LBZ, i.e., (1) coarse grain HAZ heated up to above 1250°C by subsequent pass: CGHAZ, (2) subcritically reheated CGHAZ:SRCG; (3) intercritically reheated CGHAZ:IRCG; (4) tempered IRCG heated up to above 450°C:TIRCG. All of the above four regions could be called grain coarsened zones and the API–RP2Z refers to them just as 'coarse grain zones' and makes no discrimination between the above four different microstructures **(1)**.

Relation between the critical CTOD and LBZ size

Figure 6 shows the critical CTOD versus the width of LBZ which was responsible for the crack initiation. The number of data shown are limited to those which were clearly identified to be crack initiation sites from the observation on the photo-macrographs. As a function of width of LBZ, the experimental data shows a general trend that δ_c decreases with increase in LBZ size but with a considerable scatter which implies that the individual data of CTOD is resulted from a certain probabilistic process. Figure 7 shows CTOD versus maximum LBZ size which shows again considerable scatter. Figure 8 shows CTOD versus total of the individual size of LBZ which shows more or less similar tendency to Figs 6 and 7. It may be concluded that none of three data presentations is evidently superior to the other two.

Probabilistic analysis and proposed model

Figure 9 schematically illustrates a proposed probabilistic model of HAZ CTOD which includes LBZs. It is assumed that there is a relationship between the mean CTOD ($\bar{\delta}_c$) versus the individual size of LBZ(l) as shown in Fig. 9, i.e., the mean value of CTOD may be expressed by an analytical function of LBZ size, and another assumption made is that CTOD can be approximated by the two parameter Weibull-type distribution with constant shape parameter. The relation between the mean CTOD and the LBZ size is deduced from the weakest link model assuming the CTOD distribution can be represented by the Weibull distribution **(7)** as follows.

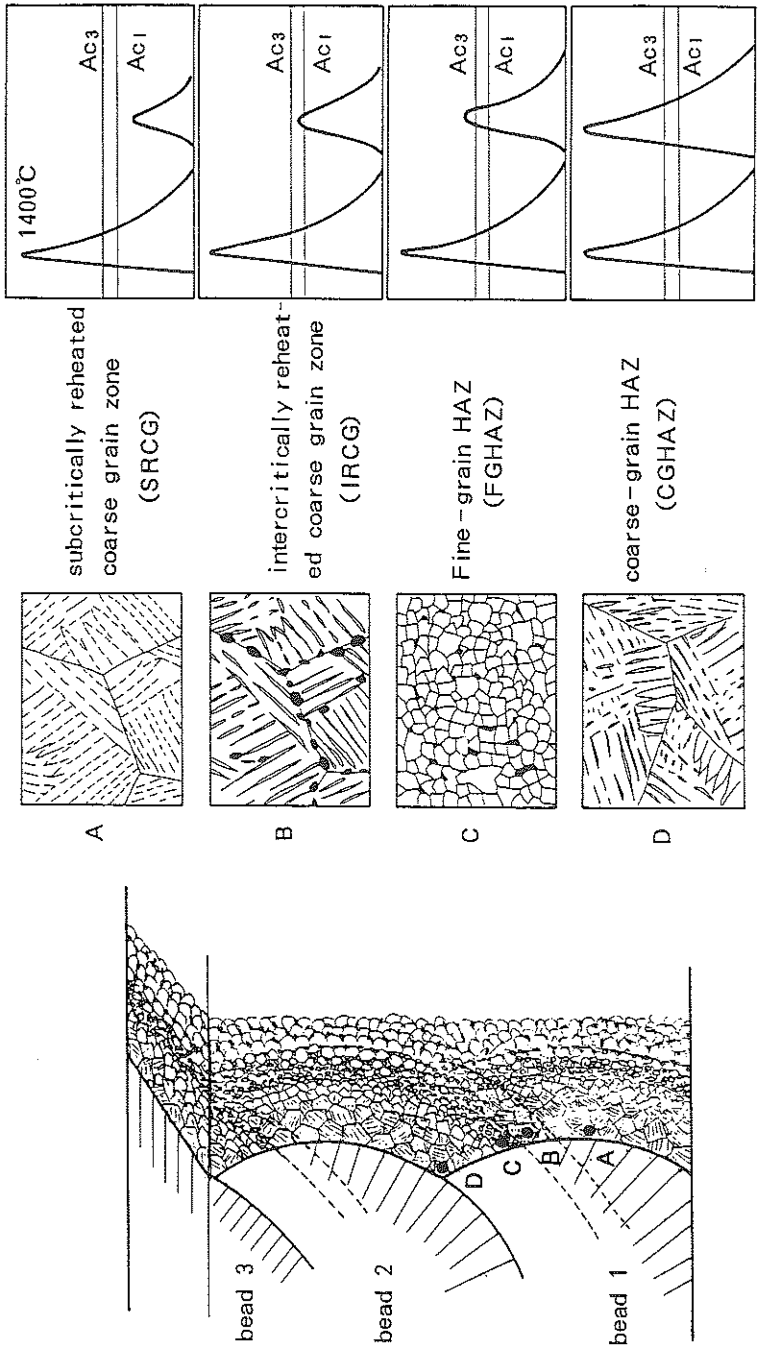

Fig 5 Schematic illustration of microstructures generated by heat cycle by welding

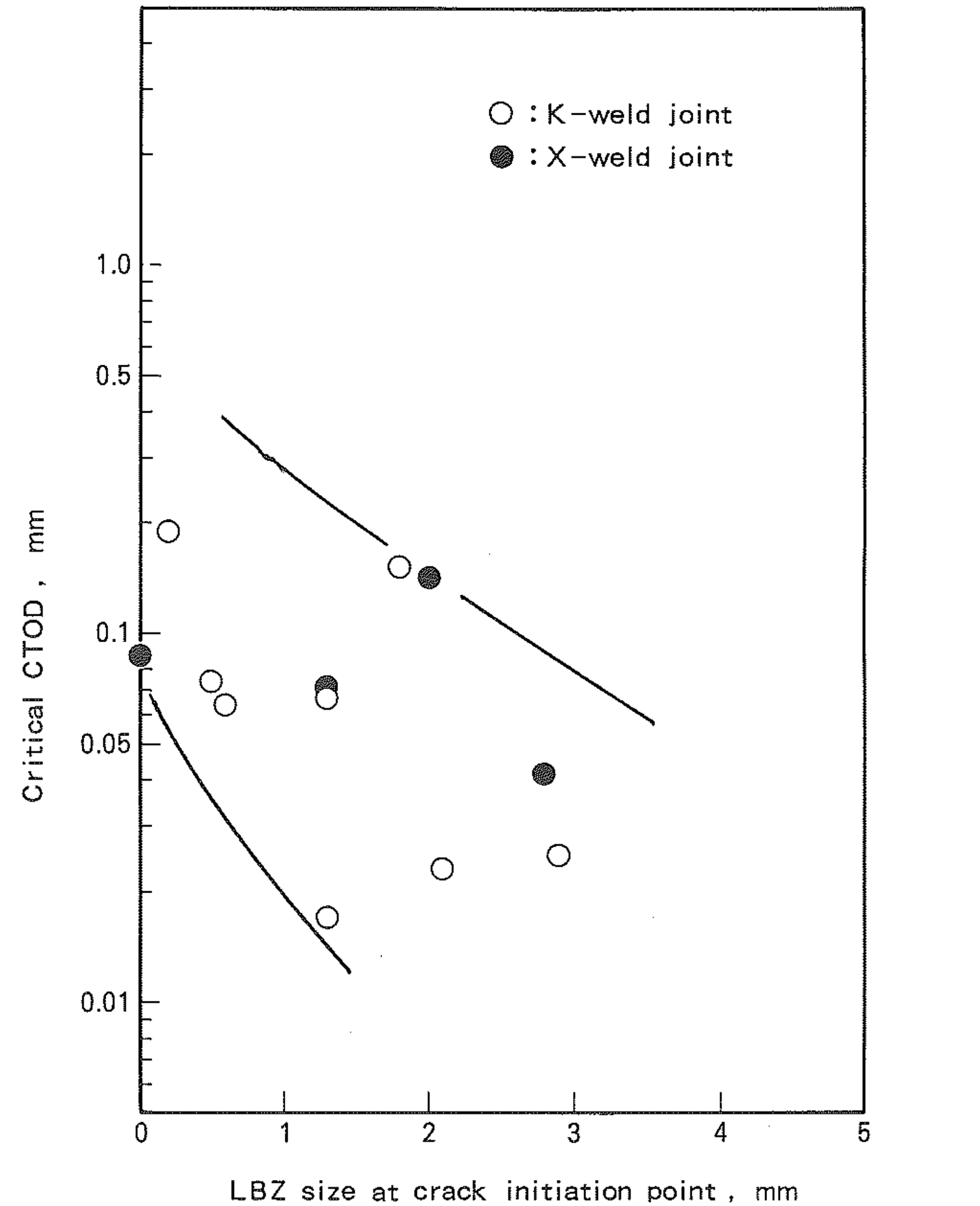

Fig 6 Critical CTOD versus LBZ size at crack initiation point

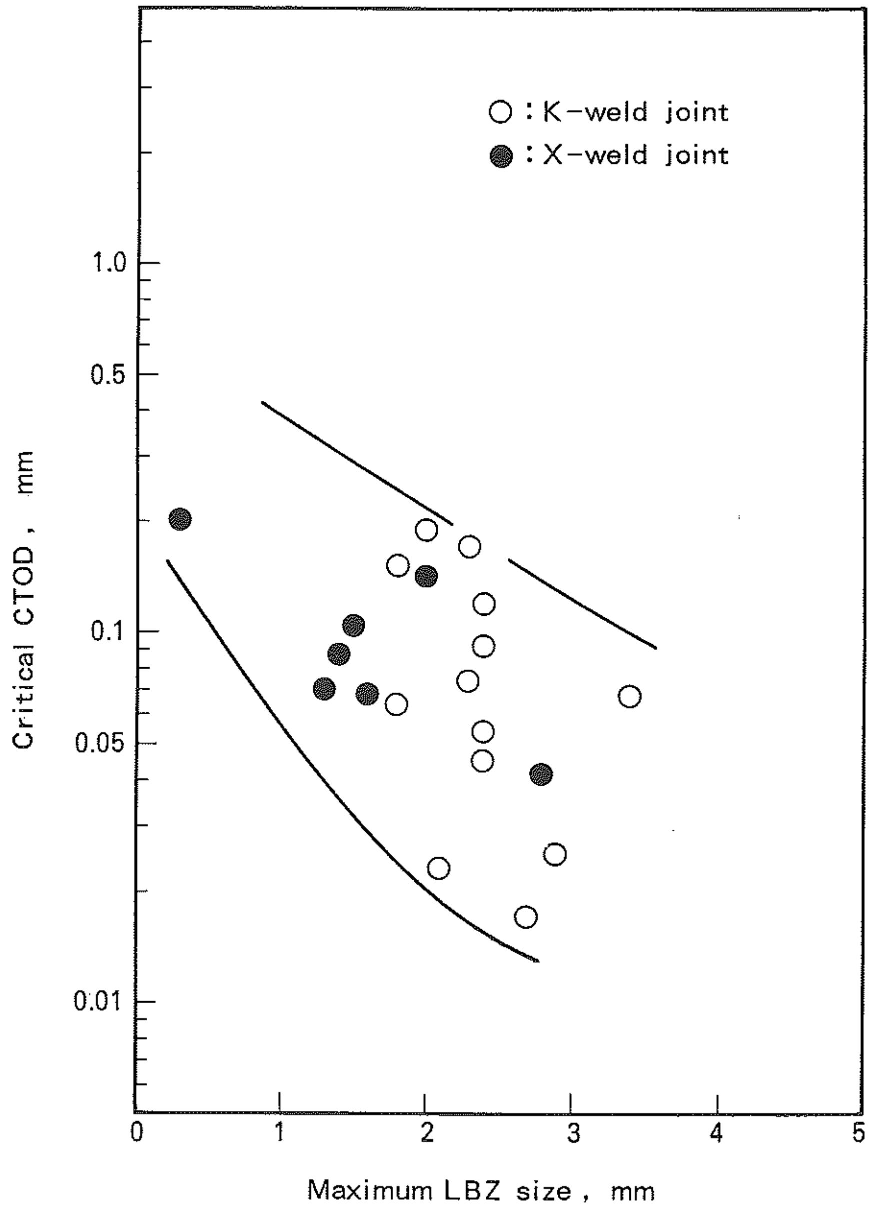

Fig 7 Critical CTOD versus maximum LBZ size

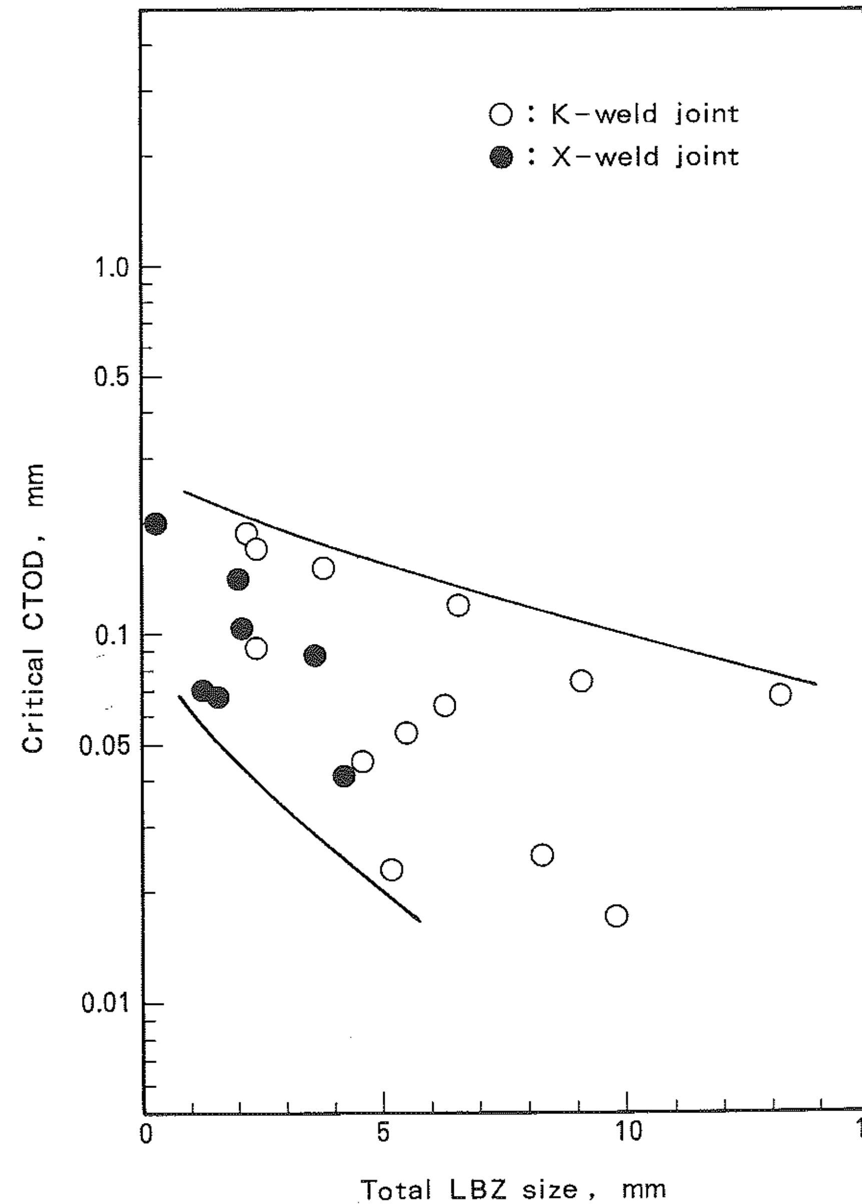

Fig 8 Critical CTOD versus total LBZ size

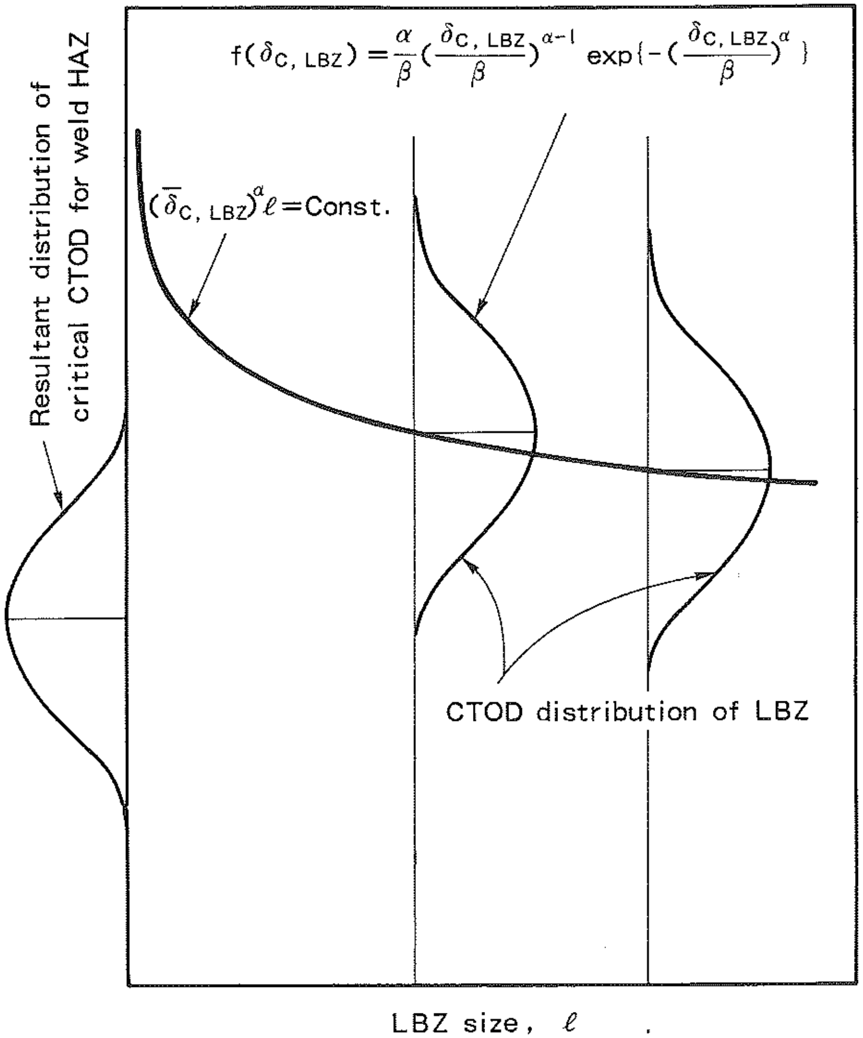

Fig 9 Proposed probabilistic model (schematic)

Consider two LBZs with size of l_1 and l_2 ($l_2 > l_1$), and assume that the probability of the occurrence of fracture below the value δ_c for LBZ with size l_2 can be expressed in terms of the probability distribution function for LBZ with size l_1 on the basis of the weakest link concept as

$$F_2(\delta_c) = 1 - \{1 - F_1(\delta_c)\}^{l_2/l_1} \tag{2}$$

where

$F_1(\delta_c)$ = probability distribution function of LBZ with size l_1
$F_2(\delta_c)$ = probability distribution function of LBZ with size l_2

Let $F_1(\delta_c)$ be the Weibull distribution expressed by

$$F_1(\delta_c) = 1 - \exp\left\{-\left(\frac{\delta_c}{\beta_1}\right)^{\alpha_1}\right\} \tag{3}$$

Then substituting equation (3) into equation (2), $F_2(\delta_c)$ is expressed by

$$F_2(\delta_c) = 1 - \exp\left\{\frac{l_2}{l_1}\left(\frac{\delta_c}{\beta_1}\right)^{\alpha_1}\right\} = 1 - \exp\left\{-\left(\frac{\delta_c}{\beta_2}\right)^{\alpha_2}\right\} \tag{4}$$

where

$$\alpha_2 = \alpha_1 (= \alpha) \quad \text{and} \quad \beta_2 = \beta_1 \Big/ \left(\frac{l_2}{l_1}\right)^{1/\alpha_1} \tag{4a}$$

From equation (4a)

$$\beta_1^{\alpha} l_1 = \beta_2^{\alpha} l_2 = \text{constant} \tag{5}$$

Because

$$\bar{\delta}_c = \beta\Gamma\left(1 + \frac{1}{\alpha}\right) \tag{6}$$

Equation (5) is equivalent to

$$(\bar{\delta}_{c,\mathrm{LBZ}})^{\alpha} \cdot l = \text{constant} \tag{7}$$

where $\bar{\delta}_{c,\mathrm{LBZ}}$ = the mean critical CTOD as a function of LBZ size l.

For HAZ CTOD specimen having varied number and size of LBZ, each LBZ gives its own δ_c value. It is assumed that among various δ_c values corresponding to individual LBZ, the smallest value controls the overall behaviour for the specimen, i.e. experimentally obtained δ_c. The distribution of this δ_c is schematically shown on the ordinate of Fig. 9 termed as 'Resultant distribution of critical CTOD for weld HAZ', which happened to be approximated by a two parameter Weibull distribution again as shown in Fig. 3, although this distribution cannot be deduced theoretically. But apparently the data imply that the Weibull distribution with three parameter will better fit to the experimental data, which is more rational from physical viewpoint.

As mentioned above when we assume the weakest link concept taking account of individual, maximum, and total LBZ sizes, the resultant marginal distribution of CTOD (δ_c) may be represented as shown on the ordinate of Fig. 9. The resultant probability distribution function of the critical CTOD for weld HAZ can be approximated by

$$F(\delta_c) = 1 - \exp\left\{-\left(\frac{\delta_c}{\beta'}\right)^{\alpha'}\right\} \tag{8}$$

Figures 10 and 11 show frequency distribution of the number of LBZ and the size of LBZ hit by fatigue pre-cracking for the 'K' weld joint, each figure

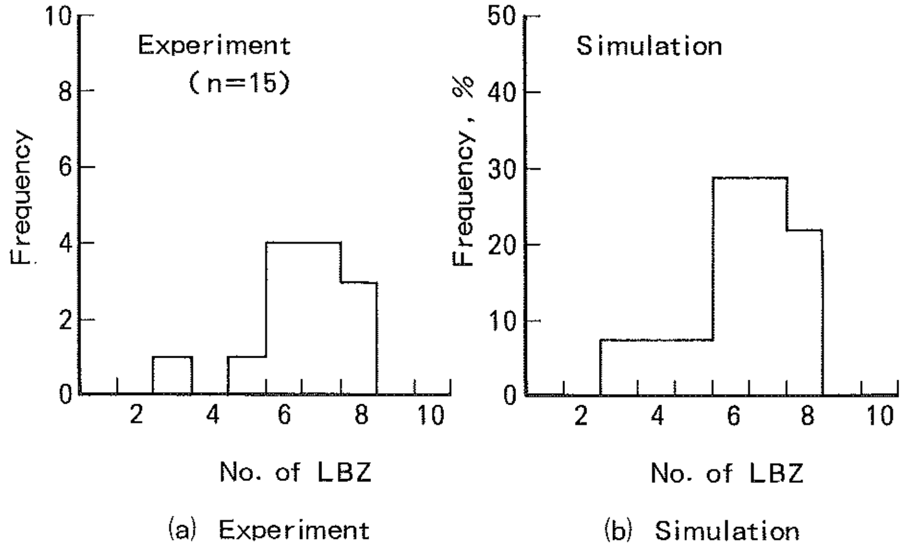

Fig 10 Frequency distribution of the number of LBZ ('K' weld joint)

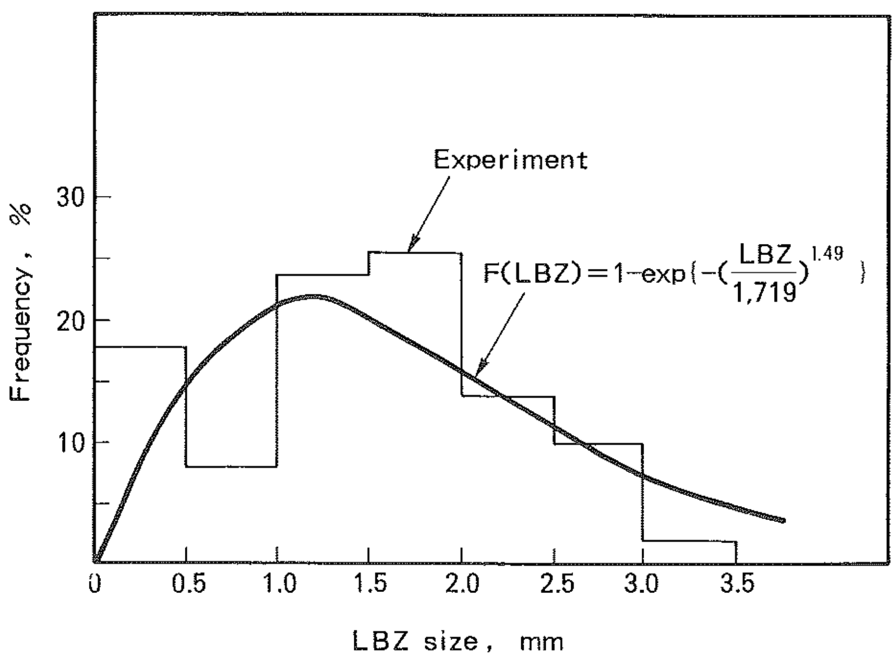

Fig 11 Frequency distribution of LBZ size ('K' weld joint)

shows the experimentally obtained data as well as the idealised relative frequency distribution used for numerical simulations, respectively. In the above mentioned simulation model, only CGHAZ, SRCG and IRCG are considered as LBZs, and discrimination between toughness level of these three regions was hard to make because of small number of experimental data. Moreover the test temperature of −60°C is the transition temperature obtained from a series of conventional 3PB HAZ CTOD tests, and this temperature is probably so low for LBZs that toughness levels are in the lower shelf toughness which are almost same among different LBZs. The TIRCG will be considered later because tempering is considered to improve toughness considerably.

Numerical simulations (Monte Carlo simulation)

Figure 12 shows the Weibull plot of 12 experimental results of CTOD testing on the 'K' joint comparing with 2000 numerical simulations where LBZ defined

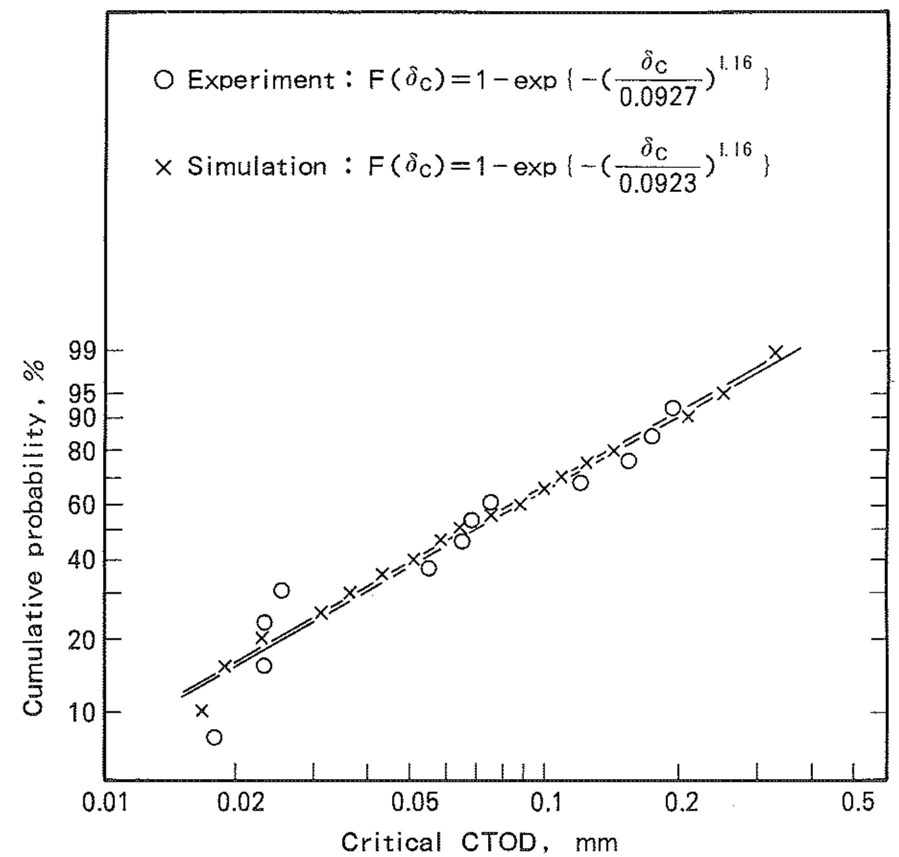

Fig 12 Comparison of Weibull plot of the critical CTOD from experiment and simulation (LBZ = CGHAZ, SRCG, IRCG)

as grain coarsened regions i.e., CGHAZ, SRCG, and IRCG, both showing almost the same Weibull distribution with $\alpha = 1.16$ (same for both results), and $\beta = 0.927$ mm and 0.923 mm for the experiments and the numerical simulations, respectively. Anyway, the difference between the experiments and the numerical simulations is very small, showing the proposed model represents a good model to predict HAZ CTOD versus size of LBZs (CGHAZ, SRCG, IRCG).

In Fig. 13 the first 200 critical CTOD data out of 2000 data generated by Monte Carlo simulations are plotted against LBZ size defined as total of the individual LBZ size based upon the above mentioned model, showing very wide scatter but mean trend of decreasing CTOD as LBZ size increases. Figure 14 shows a result but LBZ size was taken as LBZ size of crack initiating point when it was clearly identified. The results of 2000 numerical simulations are shown as mean value of $\delta_c(\bar{\delta}_c)$, and 95 percent and 90 percent lower confidence limits ($\delta_{c.5}$, $\delta_{c.10}$) together with experimental data. Figure 15 shows a similar result for δ_c versus maximum LBZ size. Figure 16 shows δ_c versus total size of LBZ. Any of the above three numerical simulations show a very big scatter of the critical CTOD which may pose a practical difficulty to make a conservative estimation of CTOD value from relatively small number of specimens. Thus 95 percent and 90 percent lower confidence limits obtained from 2000 numerical simulations may make a reference for the conservative estimation of lower limit of weld HAZ CTOD from a small number of specimens. This observation may have an association with the experimentally known fact that the lower bound critical CTOD values seen have almost no relationship with the LBZ size.

Unfortunately, the number of experimental results are small (8–11 data), it is difficult to make clear evaluation of the validity of the proposed model. When the LBZ size is small, say less than about 1.5 mm, the size of LBZ at crack initiating point seems to determine the critical CTOD, but when the LBZ size is relatively large, say larger than 1.5 mm, maximum LBZ size and total LBZ larger than 5 mm seem to give good estimation of mean CTOD. As far as lower bound estimations (90 or 95 percent confidence limits) are concerned, LBZ size at crack initiating point gives the lowest, and whereas maximum LBZ size give higher estimation particularly when the LBZ size is small, say less than 1 mm, but for total LBZ size lower confidence limits estimation may be too conservative when total LBZ size is less than say 4 mm.

Effect of tempering

Even if the TIRCG is included in the LBZs, a similar procedure can be applied, but it was clarified (8) that tempering above 450°C improves the fracture toughness considerably but the amount of toughness increase depends on the chemical composition and the tempering temperature. In reference (8), the third heating above 450°C was defined as 'tempered'. It is assumed for simpli-

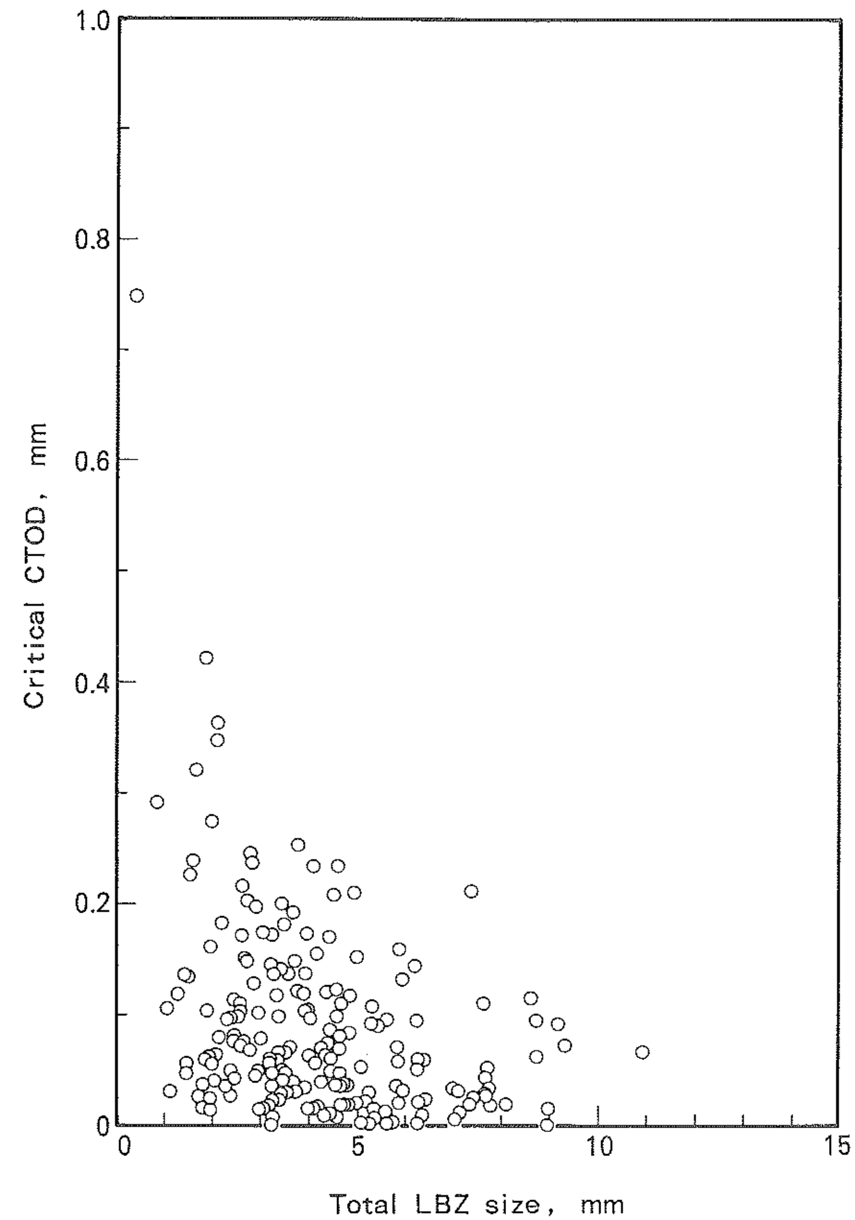

Fig 13 Results of Monte Carlo simulation of HAZ CTOD plotted against total LBZ size

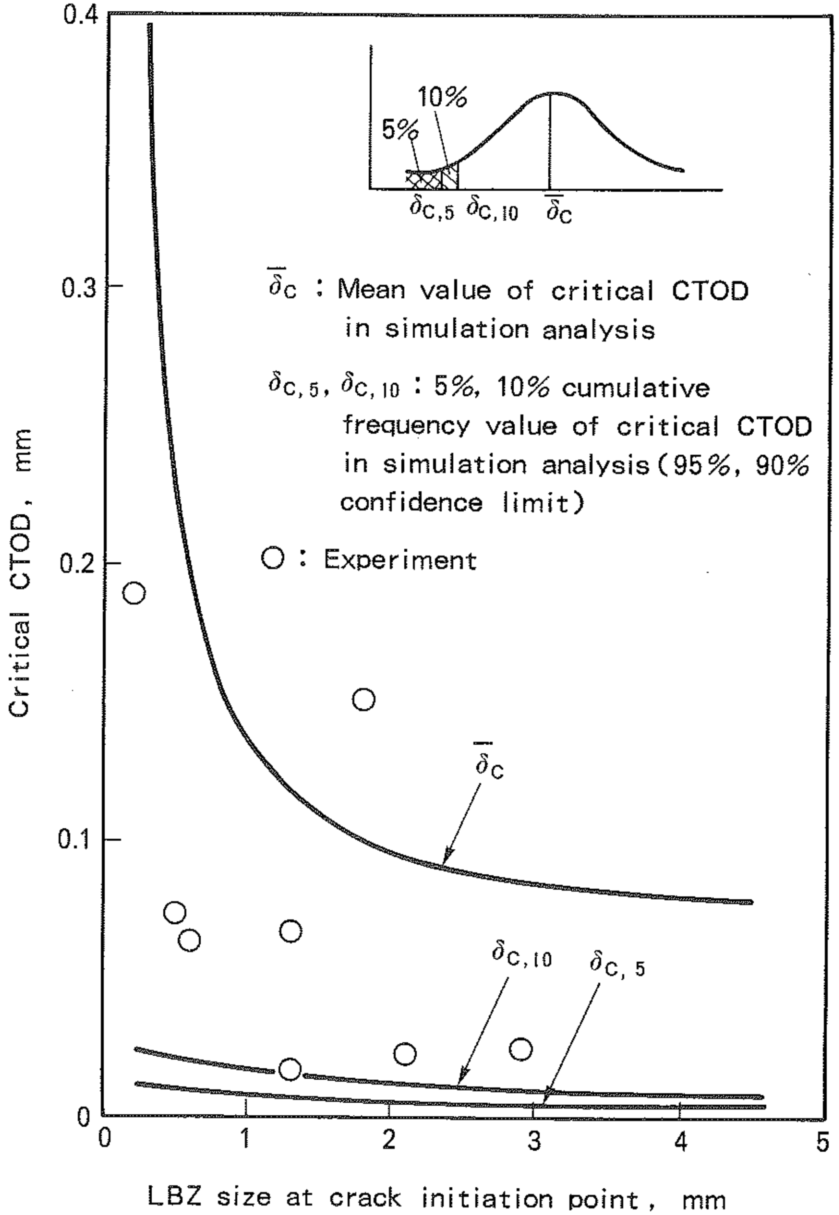

Fig 14 Comparison of critical CTOD versus LBZ size at crack initiation point between experimental and numerically simulated data (the result of simulations are presented in terms of $\bar{\delta}_c$, 90 percent and 95 percent lower confidence limit ($\delta_{c.10}$, $\delta_{c.5}$) derived from 2000 data)

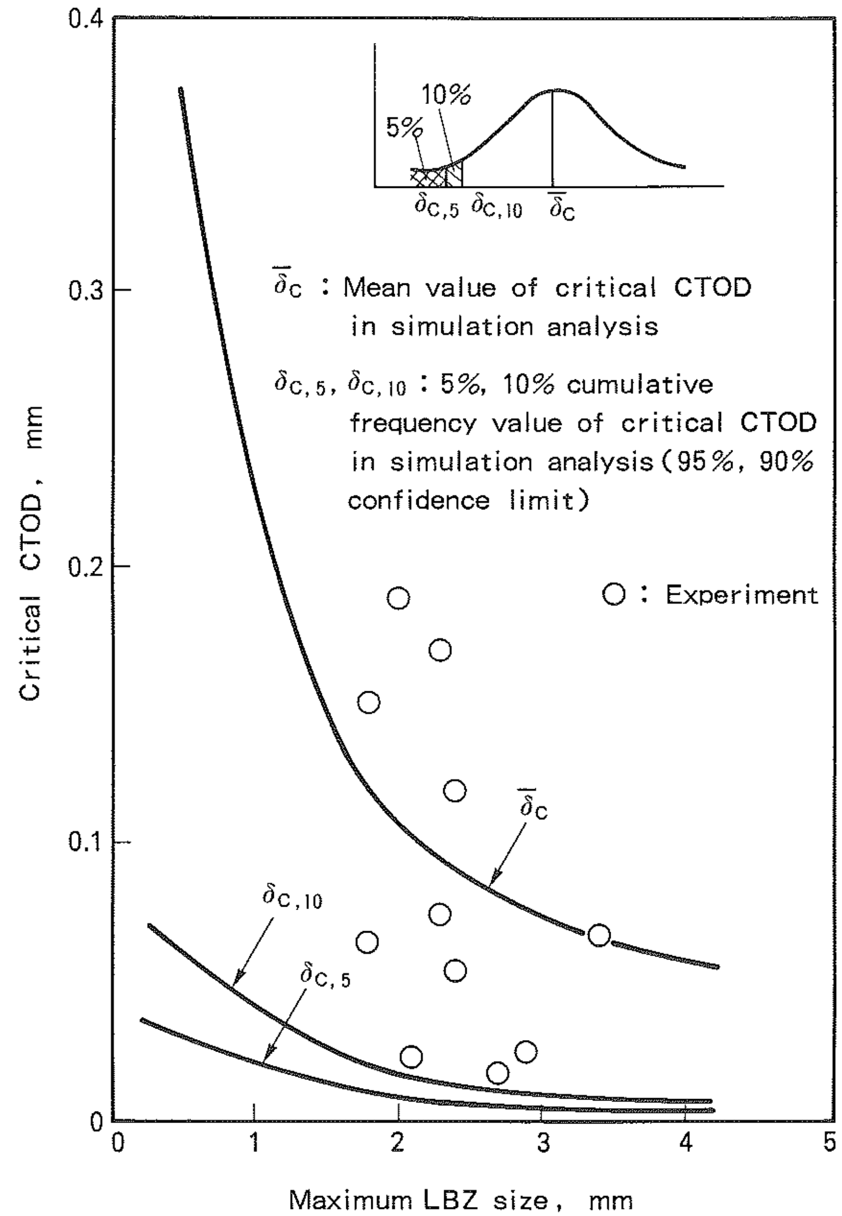

Fig 15 Data representation similar to Fig. 14 except 'LBZ size', maximum size instead of LBZ size at crack initiation point

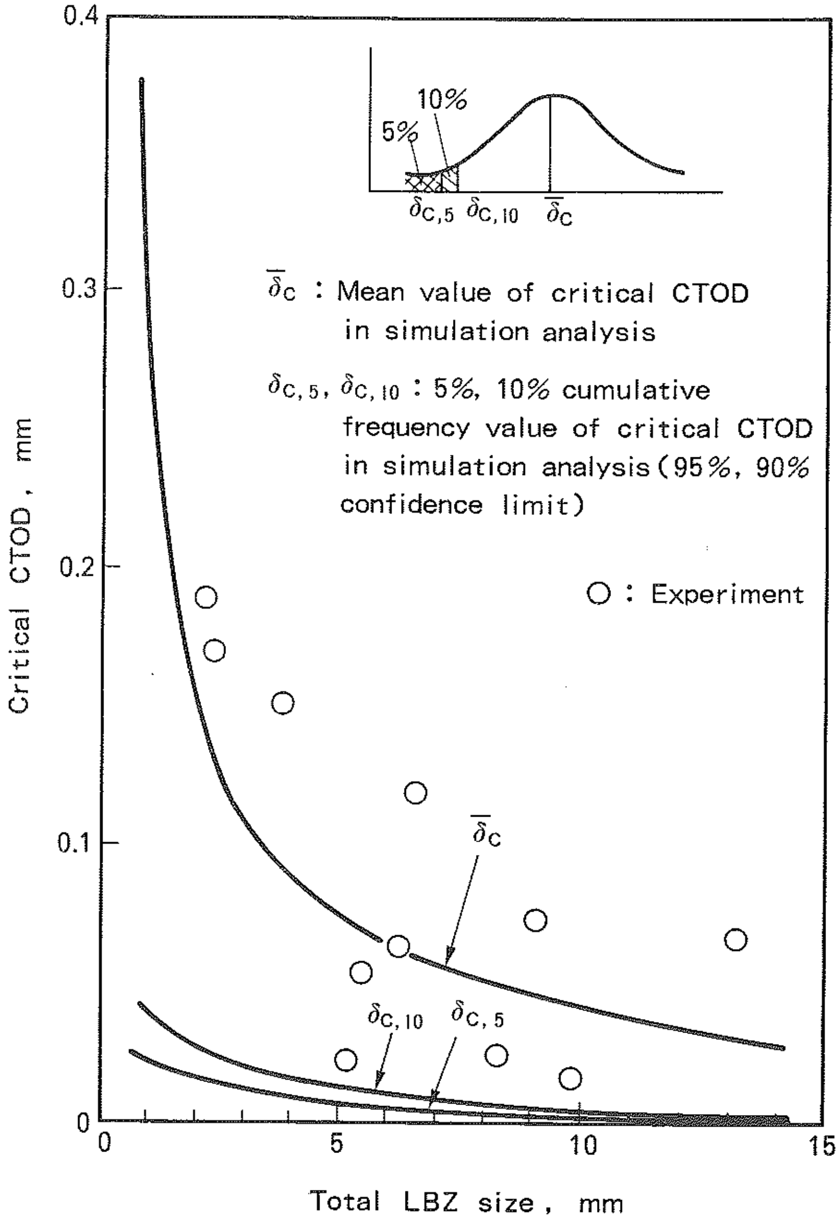

Fig 16 **Data representation similar to Fig. 14 except 'LBZ size', total of individual LBZ size instead of LBZ size at crack initiation point**

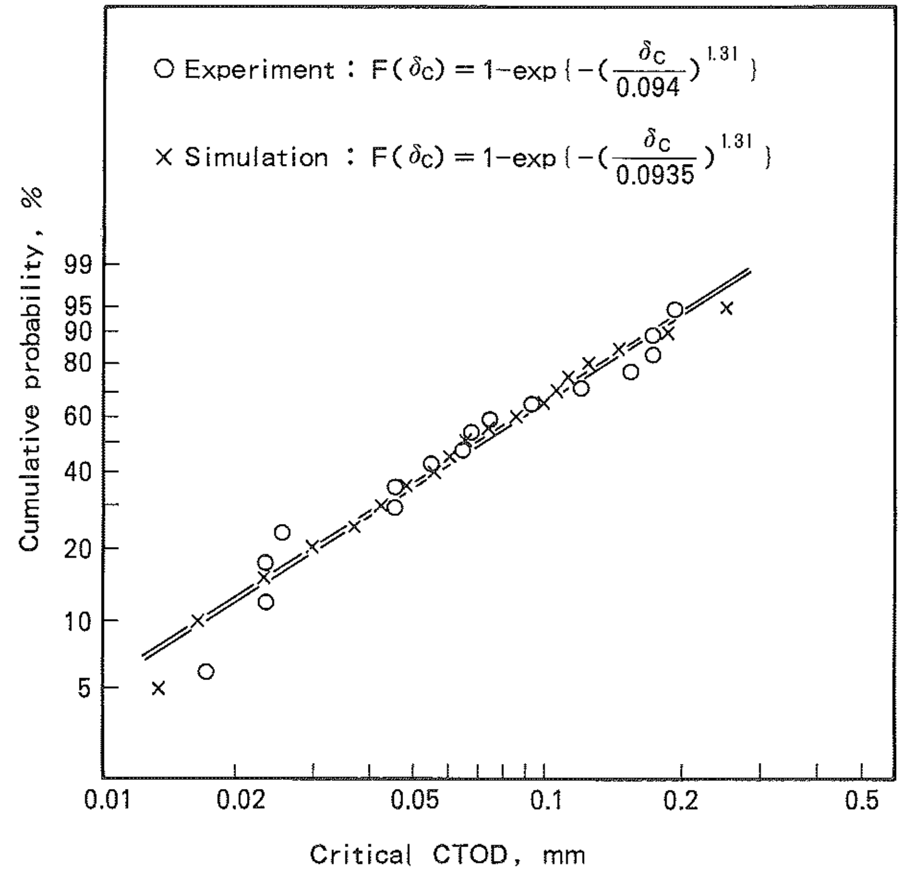

Fig 17 **Comparison of Weibull plots of critical CTOD from experimental and simulations (LBZ = CGHAZ, SRCG, IRCG, TIRCG)**

city that TIRCG resumes its toughness up to 4 times of that without temper in terms of the mean CTOD, with the value of α' unchanged.

Figure 17 shows the Weibull plots of the experimental data and those of 2000 numerical simulations taking this time the TIRCG into the model. Both results again fit well to the Weibull distribution and the simulations are in good agreement with the experiments. Comparing with Fig. 12, the change in the Weibull parameters is small. But it is more clearly implied than Fig. 12 that the Weibull distribution with three parameters should be adopted to improve the proposed model. Figure 18 was made to consider about API RP2Z requirement that a specimen with a fatigue precracking sampling total LBZs size less than 15 percent of plate thickness is invalid. Our results of simulation show that 15 percent sampling of LBZ has probability of about 40 percent, that δ_c value is lower than those experimentally determined from

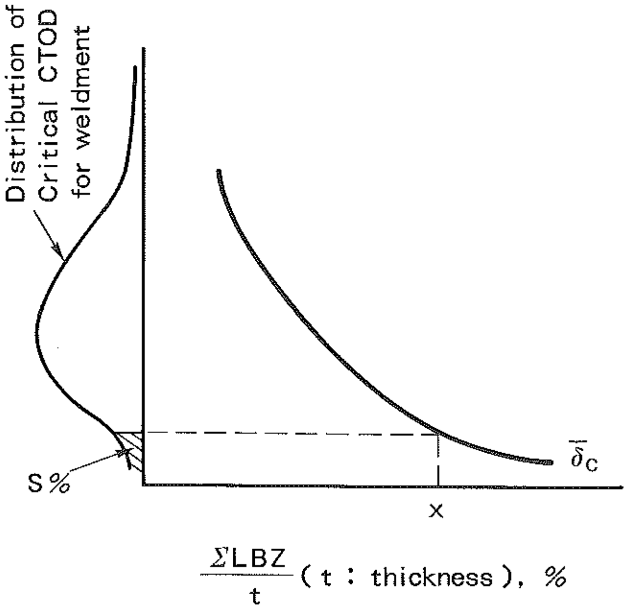

s (%)	x (%)
30.0	20.4
35.0	17.2
39.5	15.0
40.0	14.8
45.0	12.0
50.0	10.2

Fig 18 Relations between mean critical CTOD ($\bar{\delta}_c$), and PDF of δ_c versus X (relative total LBZ size to plate thickness) obtained from numerical simulation

valid testings. The value of S decreases only to 30 percent even if the value of X is increased up to 20 percent. X more than say 20 percent will give difficulties for making valid specimen. Hence, it could be suggested from the practical point of view that a kind of safety factor depending on the value of X may be used.

Figure 19 shows relation between percent CG region (X) versus δ_c normalised by $\bar{\delta}_c$ to compare the Fairchild's experimental results **(9)** with our simulation (LBZ = CGHAZ, IRCG, SRCG, TIRCG). The results of simulation gives quite similar results to those by Fairchild and a 'void area' may suggest that a specimen with percent CG region less than ~8 percent is invalid.

Effect of plate thickness

Effect of plate thickness on HAZ CTOD is twofold; one is due to triaxiality of stress state or plane strain condition, say 'mechanical effect', the other is, say 'metallurgical or statistical effect', which comes from the fact that the thicker the plate the probability of the number and size of LBZ hit by fatigue precrack will increase. Both effects results in the fact that the thicker joint tends to show lower toughness.

As for the mechanical effect, a number of theoretical and empirical expressions have been proposed. The one we adopted was derived by Kawano **(10)**.

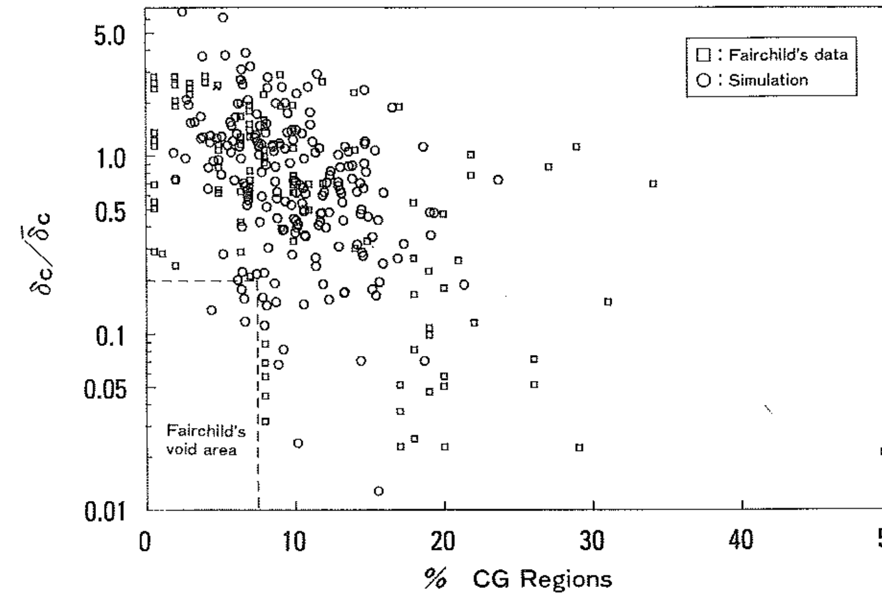

Fig 19 CTOD versus percent CG regions as compared with the data by Fairchild

The mechanical plate thickness effect on CTOD is expressed by

$$\frac{\delta_{CB}}{\delta_{c1}} = \left(\frac{2}{\sqrt{3}}\right)^{N+1} \cdot \{0.79 + \alpha(\alpha - 1.3)\}^{N-1/2} \cdot \left(0.85 - \frac{\alpha}{2}\right)/0.7^N$$

where

$\alpha = (1 - \gamma)/2$, $\gamma = 10.2/(B + 5.2)$, $B \geqslant 10$ mm, (B = plate thickness (mm))
δ_{c1} = CTOD for plane strain condition
δ_{CB} = CTOD for plate with thickness B mm
N = strain hardening exponent ($\varepsilon^p_{eq}/\varepsilon_Y = F \cdot (\sigma_{eq}/\sigma_Y)^N$)

Regarding the metallurgical effect, the experimentally obtained frequency distribution of the number of LBZ for 'K' joint HAZ hit by fatigue precracking is shown in Fig. 20 for 10, 25, and 50 mm thick plates, respectively. The frequency distributions for 10 and 25 mm thick plates were determined from that experimentally obtained data for 50 mm thick plate with the assumption that the welding conditions are unchanged and thus the size and distribution of LBZ are the same.

Figure 21 shows the Weibull plot of numerically simulated 2000 data for HAZ CTOD of 50, 25, and 10 mm thick plates. The shape parameter is almost the same for the varied thicknesses. For cumulative probability of 50 percent, δ_c values are 0.07, 0.18, and 0.8 mm and the values for 25 and 10 mm thick plate to that for 50 mm thick are 2.57 and 11.43, respectively, showing a quite

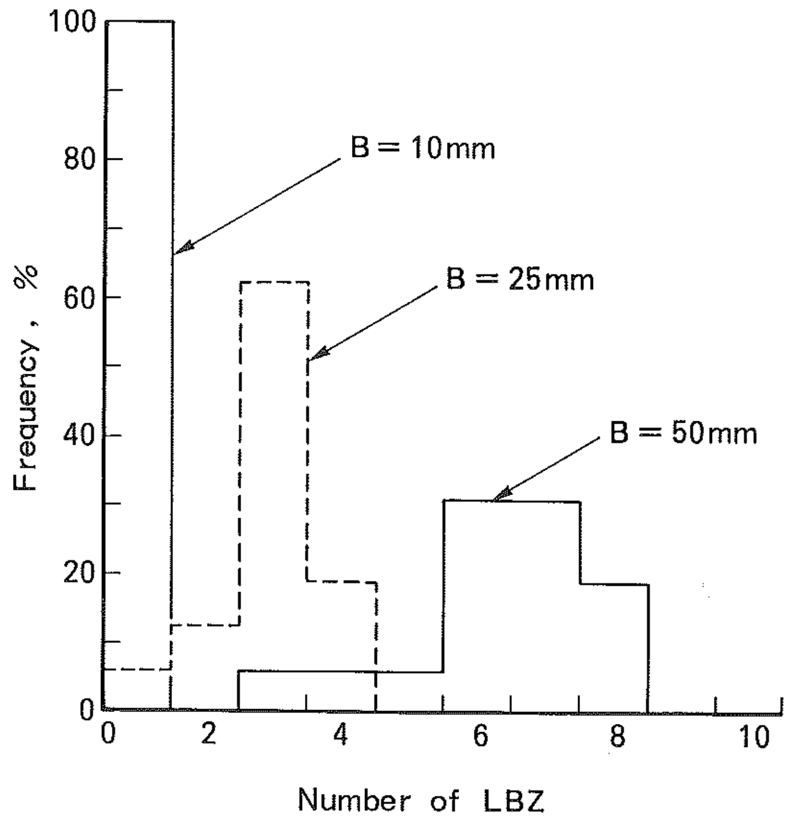

Fig 20 **Frequency distribution of number of LBZ hit by fatigue precrack for K weld joint made from 50, 25, and 10 mm thick plates**

significant plate thickness effect compared with fracture toughness of non-welded plate. If only the mechanical factor is considered, the above ratios will be 1 : 1.45 : 3.94 which reveals that in case of HAZ CTOD, plate thickness effect is controlled primarily by the metallurgical factor.

Conclusions

The HAZ CTOD data under the influence of the existence of small local brittle zone (LBZ) along the pre-crack front were statistically analysed through the numerical simulations. The proposed statistical model to analyse the effect of the LBZ on the CTOD value is based on the weakest link model with the assumption of Weibull distribution with two parameters for the toughness of the LBZ as well as probabilities of the size and the number of LBZ hit by a fatigue pre-crack front. They were determined from the heat flow analysis of

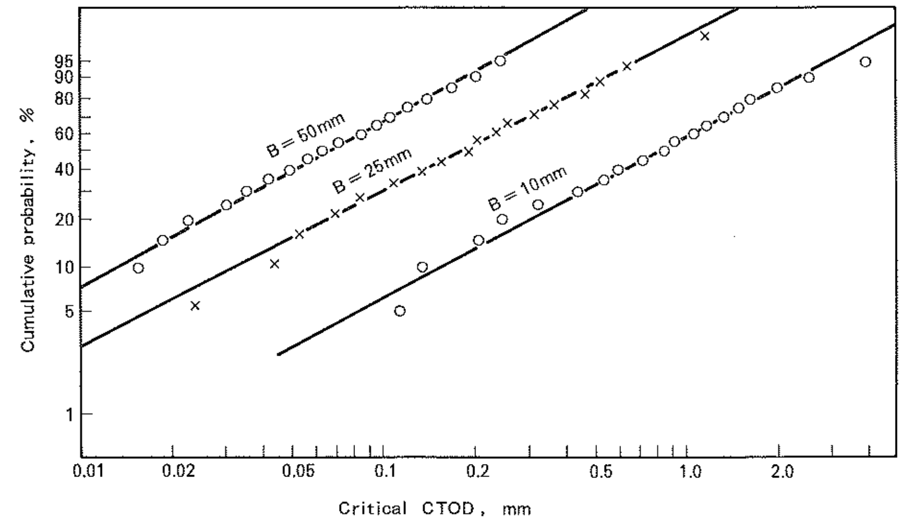

Fig 21 **Estimated effect of plate thickness on 'K' weld joint HAZ CTOD test in terms of Weibull plot from 50, 25, and 10 mm thick plates**

multi-pass weld for each specimen. Following conclusions may be drawn from the present study.

(1) A probabilistic model for the analysis of the effect of LBZ on the critical CTOD of weld HAZ was proposed. The relation between the mean CTOD and the LBZ size was deduced from the weakest link concept by assuming the two parameter Weibull distribution for the critical CTOD of LBZ. The frequency distributions of the number and the size of LBZ hit by fatigue precracking were also assumed in accordance with the empirical results. The probabilistic distributions of the experimental CTOD values, which could be approximated by again the two parameter Weibull distribution, was well explained by the numerical simulations using the proposed statistical model.

(2) The Monte Carlo simulation was carried out using the proposed probabilistic model and compared with experimental data in terms of critical CTOD versus LBZ size at crack initiation point, maximum LBZ size and total LBZ size along the pre-crack front. The numerical simulations shows the effect of LBZ size on the CTOD value, and are consistent with general trend in the experimental results. Although it is difficult to discuss in detail because of a large scatter and a lack of systematic experimental data, the proposed statistical model seems to be reasonable to explain the effect of LBZ on the CTOD of HAZ.

(3) Effect of tempering is taken into account and it was revealed the above conclusion is also valid.

(4) Numerical simulations have been carried out to clarify the meaning of API recommendation on the ratio of coarse grained zone occupied along the crack front. Present analytical results are consistent with the experimental tendency obtained by others and show the API recommendation of 15 percent on the coarse grained zone ratio to whole length of the crack front is not always conservative to get eventual low CTOD value.
(5) The effect of specimen thickness on the CTOD values of HAZ was also investigated using the statistical model taking also into account of the mechanical constraint effect. It was shown that in case of HAZ CTOD, plate thickness effect was controlled primarily by the metallurgical effect.

Acknowledgements

The present work is one of several attempts to interpret the experimental data generated by the FTW Committee of the Japan Welding Engineering Society (JWES), the main purpose of which is to draft recommendations for CTOD testing on weldments. The authors wish to extend their sincere gratitude for the Committee members' valuable discussion as well as their great assistance in carrying out the tedious experiments, particularly to Professor Toyoda and Dr Minami (Osaka University), Professor Toyosada (Kyushu University), five leading Japanese Steel manufacturers, Mitsubishi Heavy Industries Ltd, and other fabricators. The authors also express their appreciation to Dr Aihara of Nippon Steel Corporation for his useful suggestions for drafting this paper.

References

(1) *API Recommended Practice* **2Z(RP2Z)**, (1987).
(2) *Steel Specification for Offshore Structures* (EEMUA **150**), (1987).
(3) FAIRCHILD, D. P., THEISEN, J. D., and ROYER, C. P. (1988) *Proc. Int. Conf. Offshore Mech. and Arctic Engng*, ASME, Vol. **3**, p. 247.
(4) MACHIDA, S., MIYATA, T., TOYOSADA, M., and HAGIWARA, Y. Proc. symp. on fatigue and fracture testing of weldments, *ASTM STP* **1058**, 1988.
(5) PALEY, Z., LYNCH, J. N., and ADAMS, C. M. (1964) *Welding J.*, **43**, 2.
(6) HAZE, T. and AIHARA, S. (1986) IIW Doc. IX–1423–86, Tokyo.
(7) SATOH, K., TOYODA, M., and MINAMI, F. (1985) *Trans. Japan Welding Soc.*, **16**, 70.
(8) HAZE, T. and AIHARA, S. (1989) *Proc. 7th Int. Conf. Offshore Mech. and Arctic Engng*, ASME, Vol. **III**, p. 515.
(9) FAIRCHILD, D. P., Proc. symp. on fatigue and fracture testing of weldments, *ASTM STP* **2058**, 1988.
(10) KAWANO, S. (1984) *Fundamental study on plate thickness effect on fracture toughness of structural steels under large-scale yielding condition*, PhD thesis, Hiroshima University (in Japanese).